Electronic Supplementary Information for

Modulation of a coordination structure in europium(III)-based metallo-supramolecular polymers for high proton conduction

Yemineni S L V Narayana, Chanchal Chakraborty, Utpal Rana, Yoshikazu Ninomiya, Takefumi Yoshida and Masayoshi Higuchi*

Electronic Functional Macromolecules Group, National Institute for Material Science (NIMS), Tsukuba 305-0044, Japan.

E-mail: HIGUCHI.Masayoshi@nims.go.jp

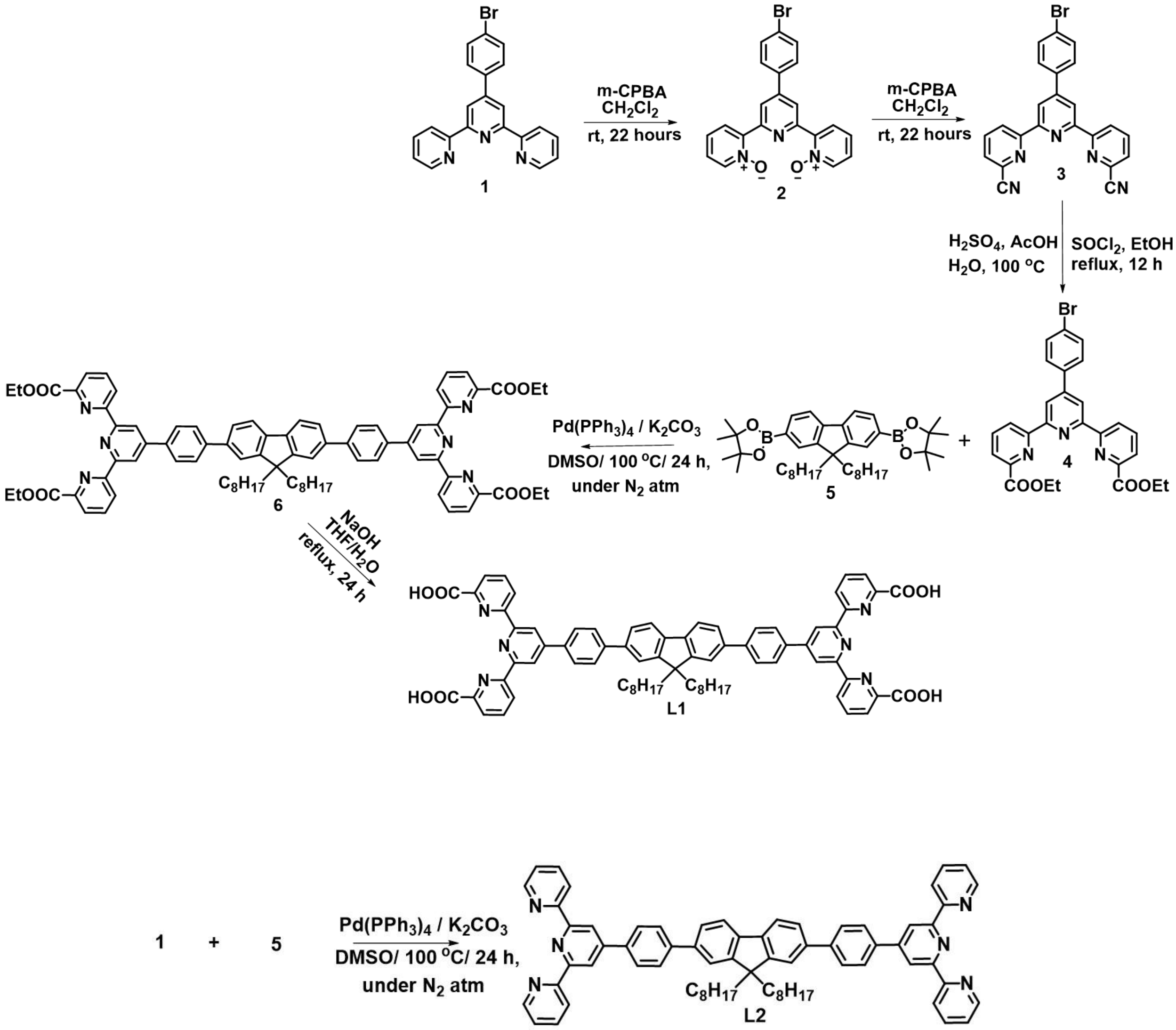

Scheme S1. Synthetic scheme for L1 and L2.

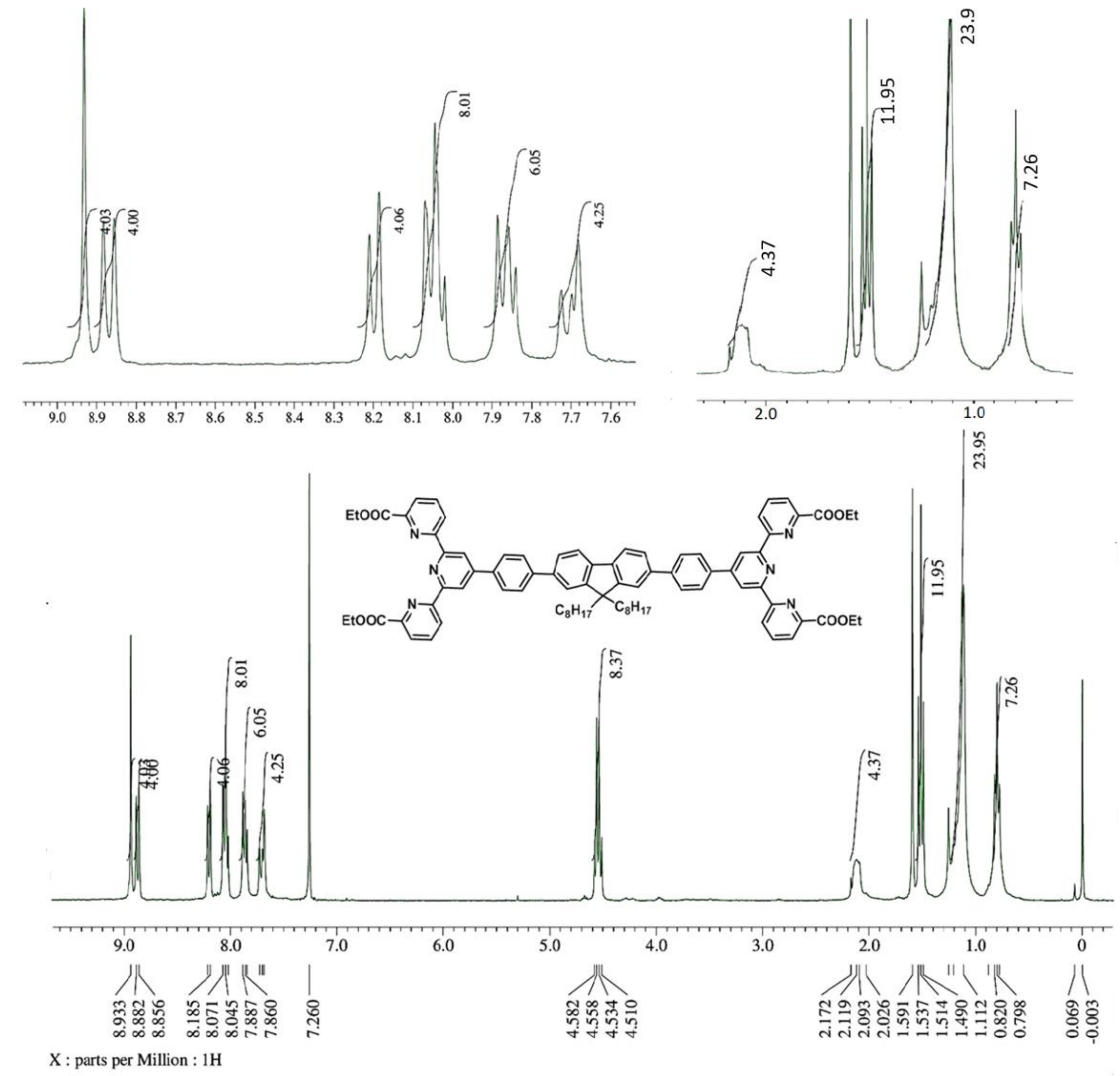

Fig. S1. ^{1}H NMR spectrum of tetra ester derivative of L1.

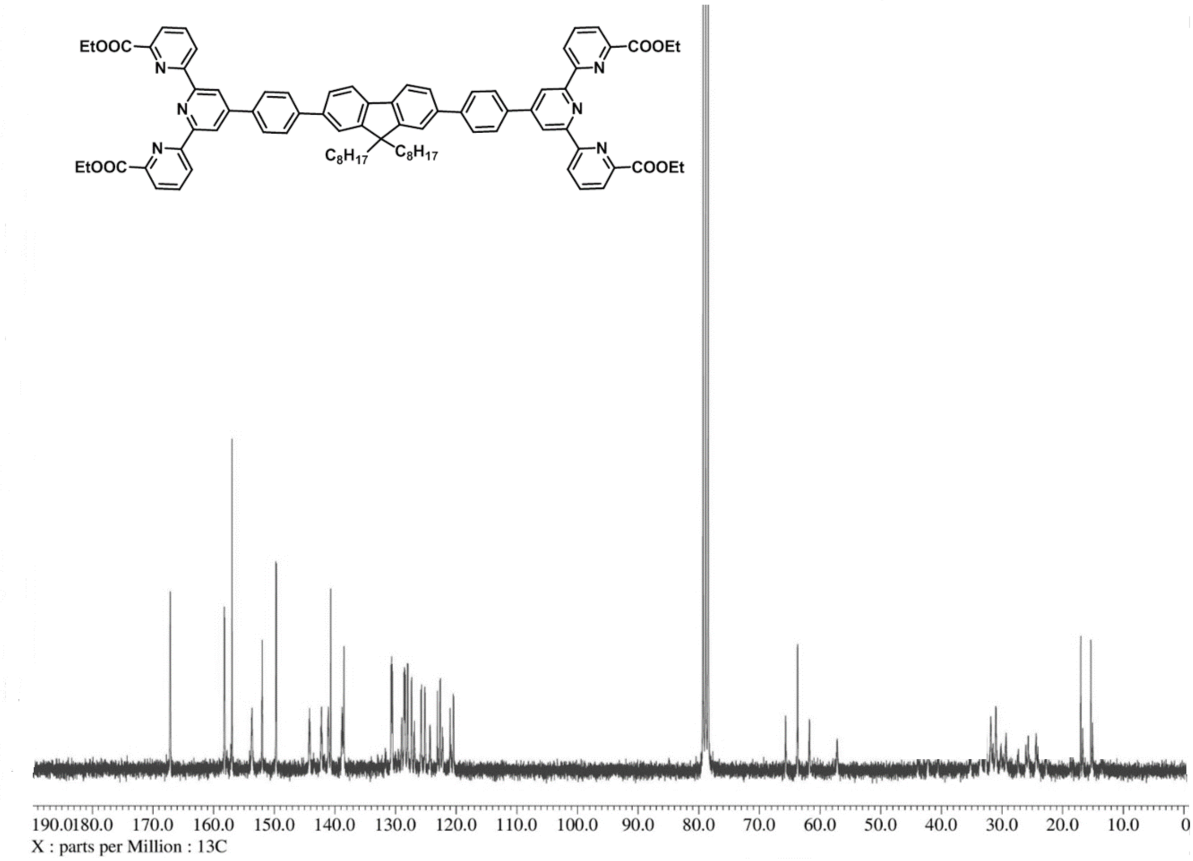

Fig. S2. ^{13}C NMR spectrum of tetra ester derivative of L1.

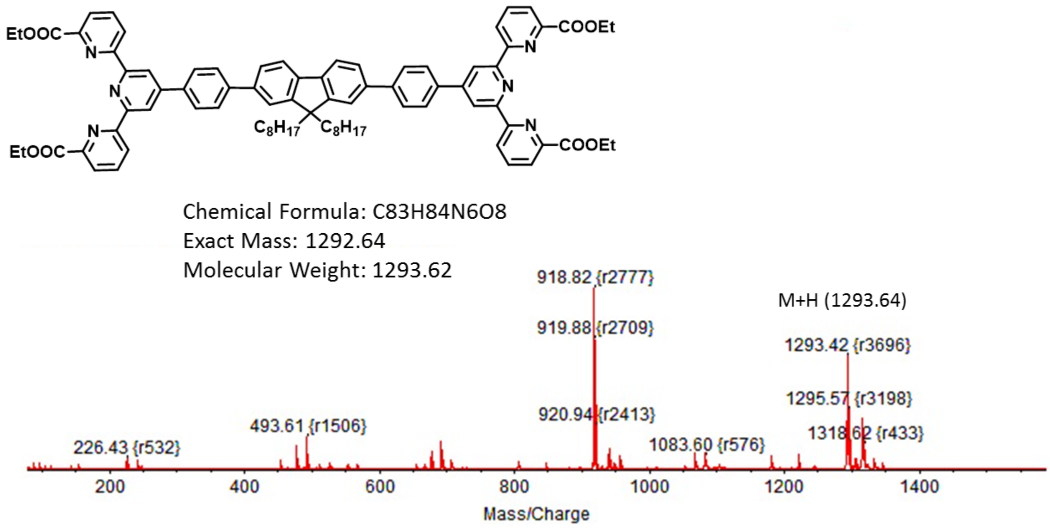

Fig. S3. MALTI-TOF spectrum of tetra ester derivative of L1.

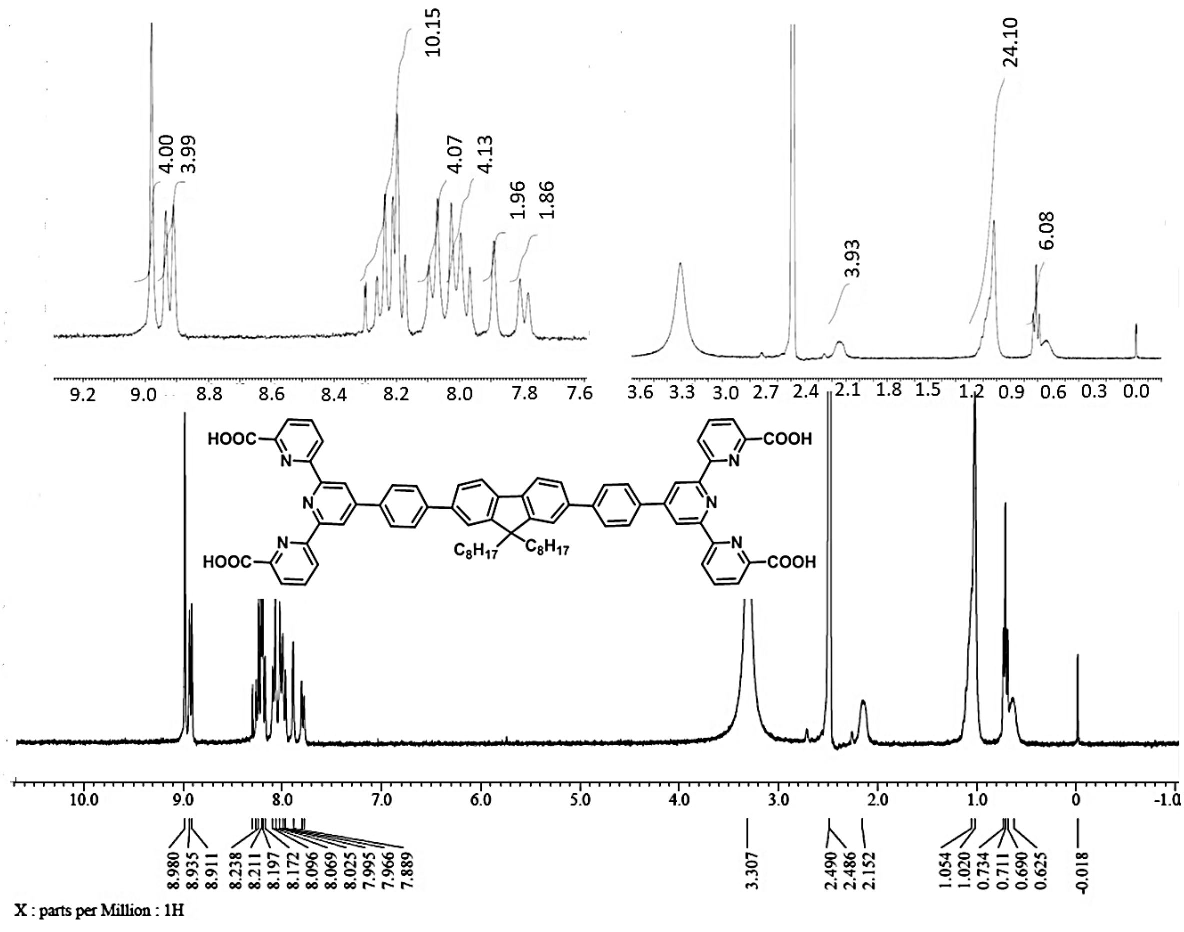

Fig. S4. ^{1}H NMR spectrum of L1.

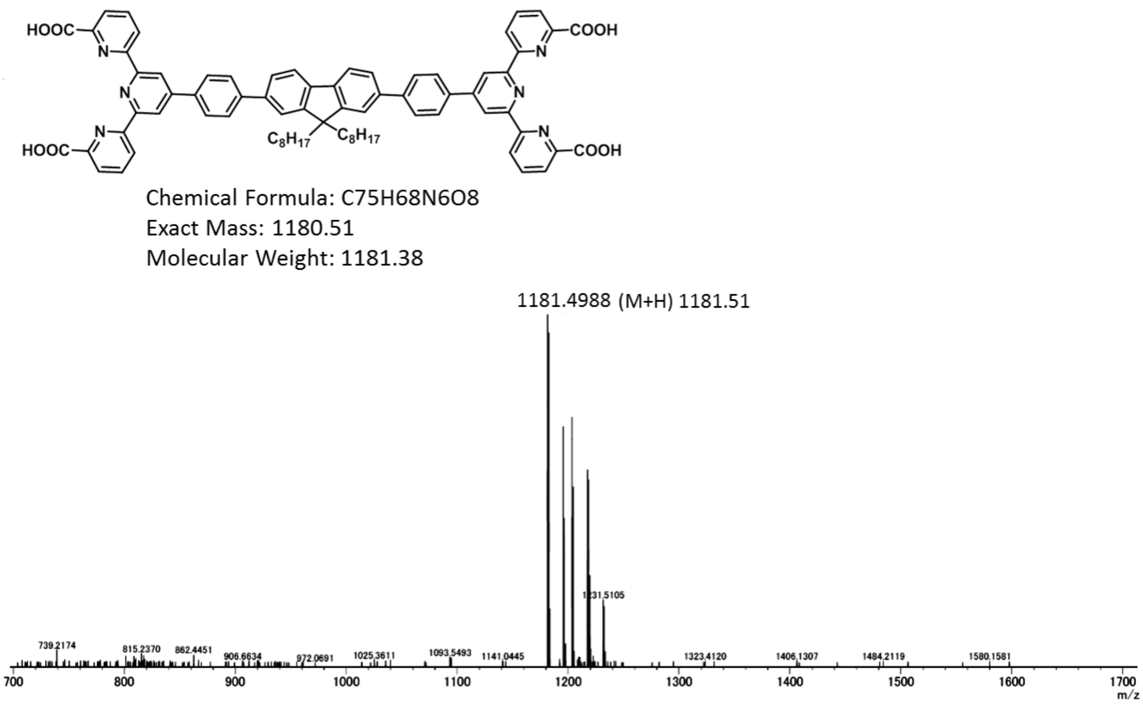

Fig. S5. HR-Mass spectrum of L1.

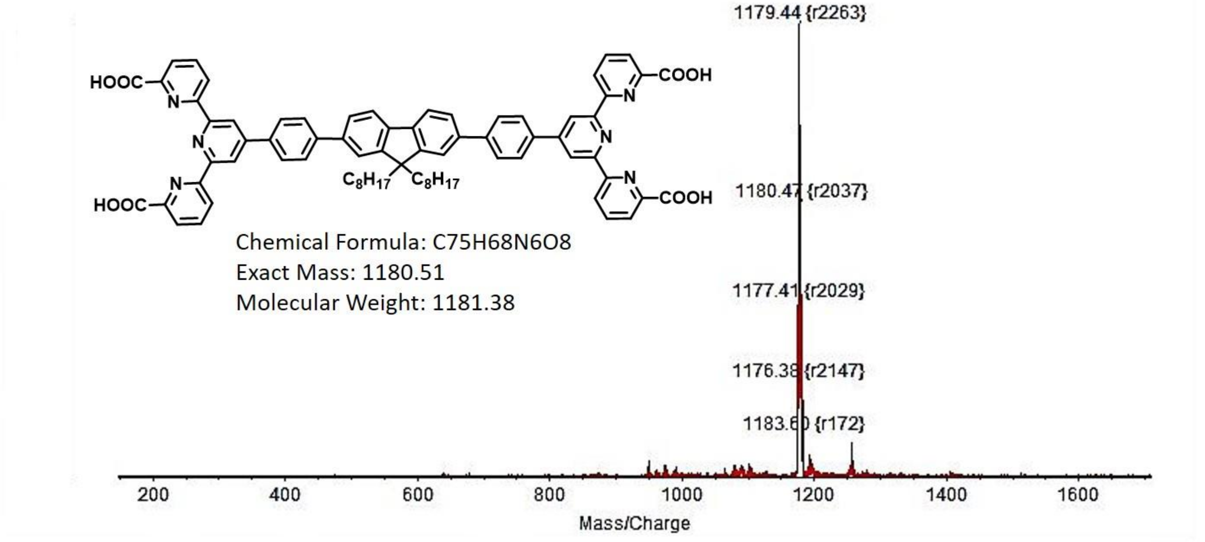

Fig. S6. MALTI-TOF spectrum of L1.

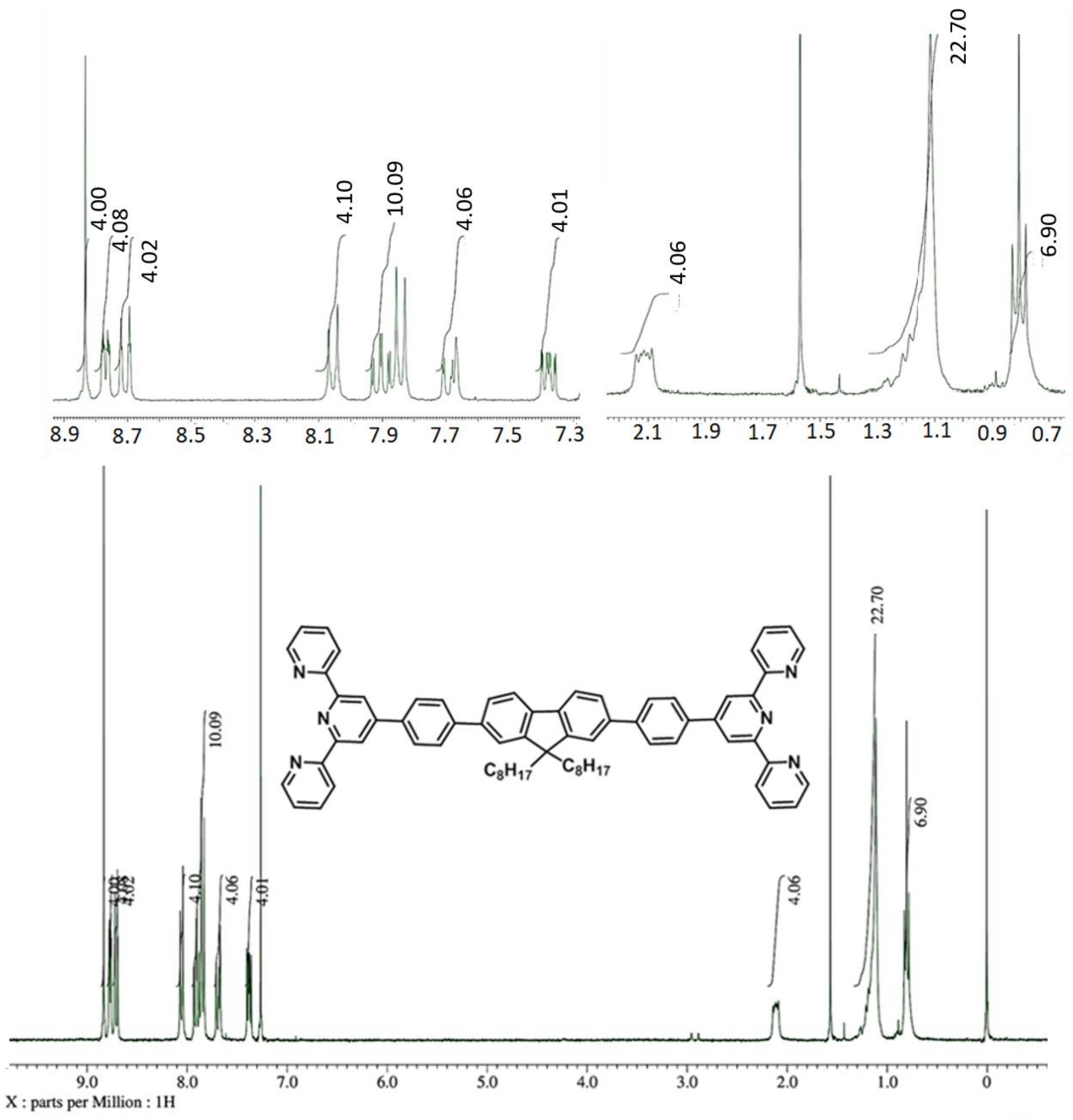

Fig. S7. ^{1}H NMR spectrum of L2.

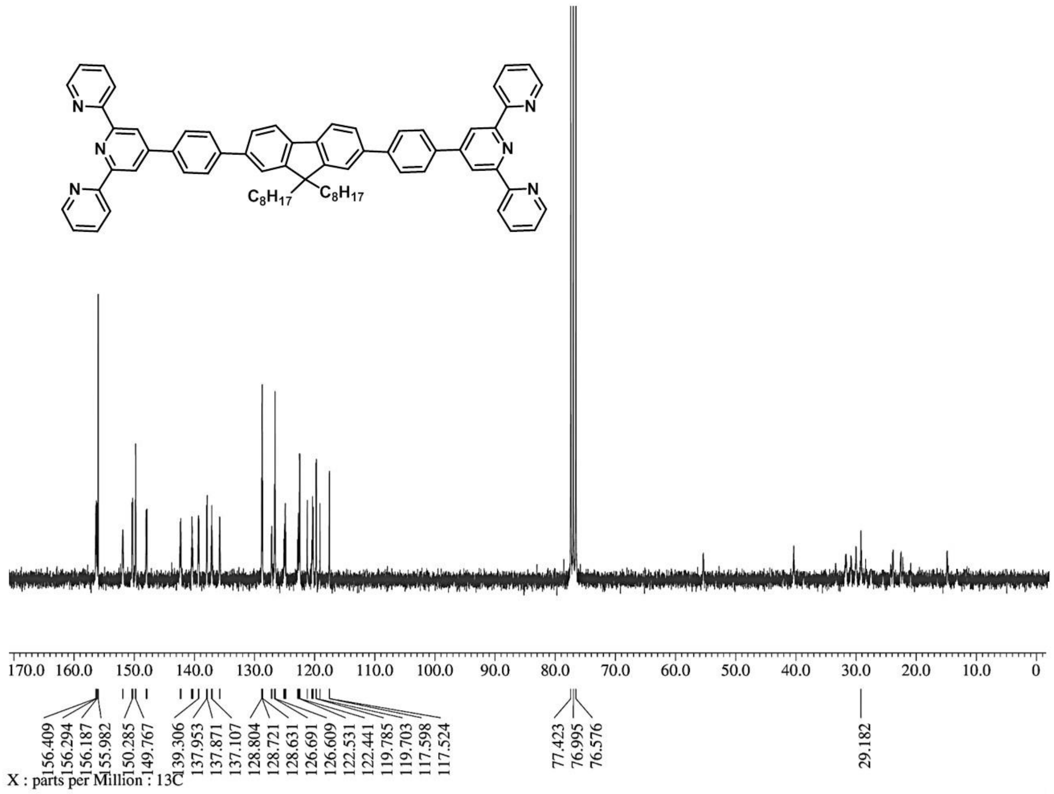

Fig. S8. ^{13}C NMR spectrum of L2.

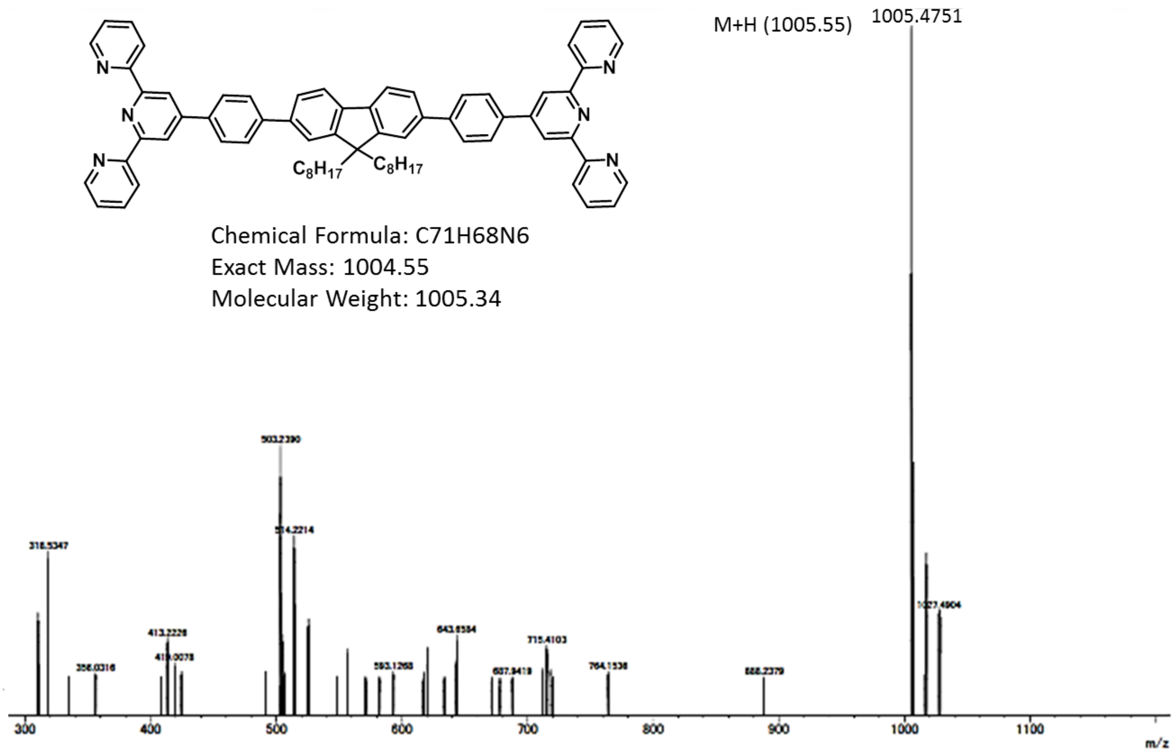

Fig. S9. HR- Mass spectrum of L2.

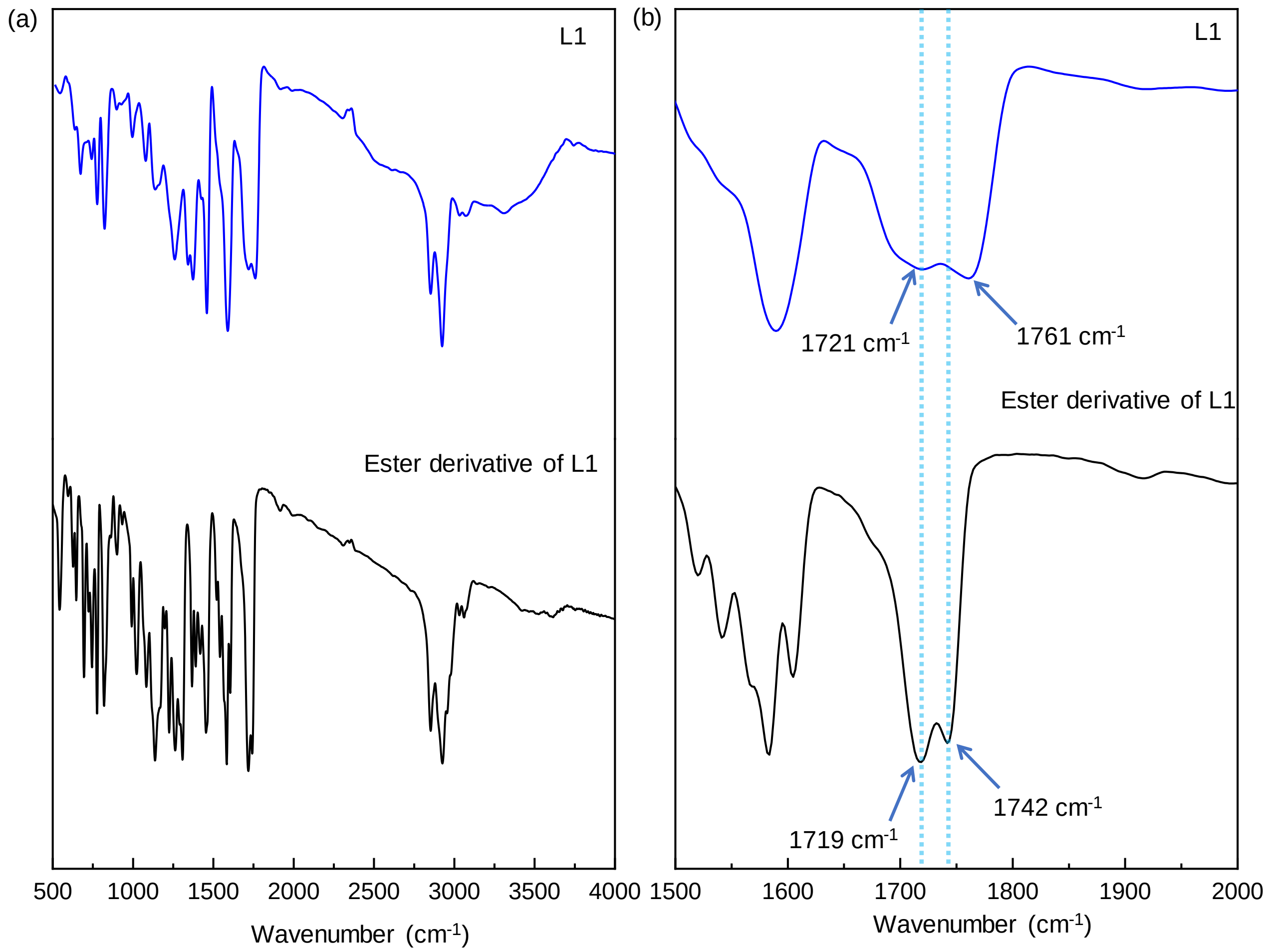

Fig. S10. FT-IR Spectra of L1 and ester derivative of L1. a) 500-4000 cm^{-1} b) 1500-2000 cm^{-1}

We showed FT-IR spectra of L1 and ester derivative of L1 in Fig. S10. C=O stretching frequency in carboxylic acid is blue shifted compared with its ester derivative.

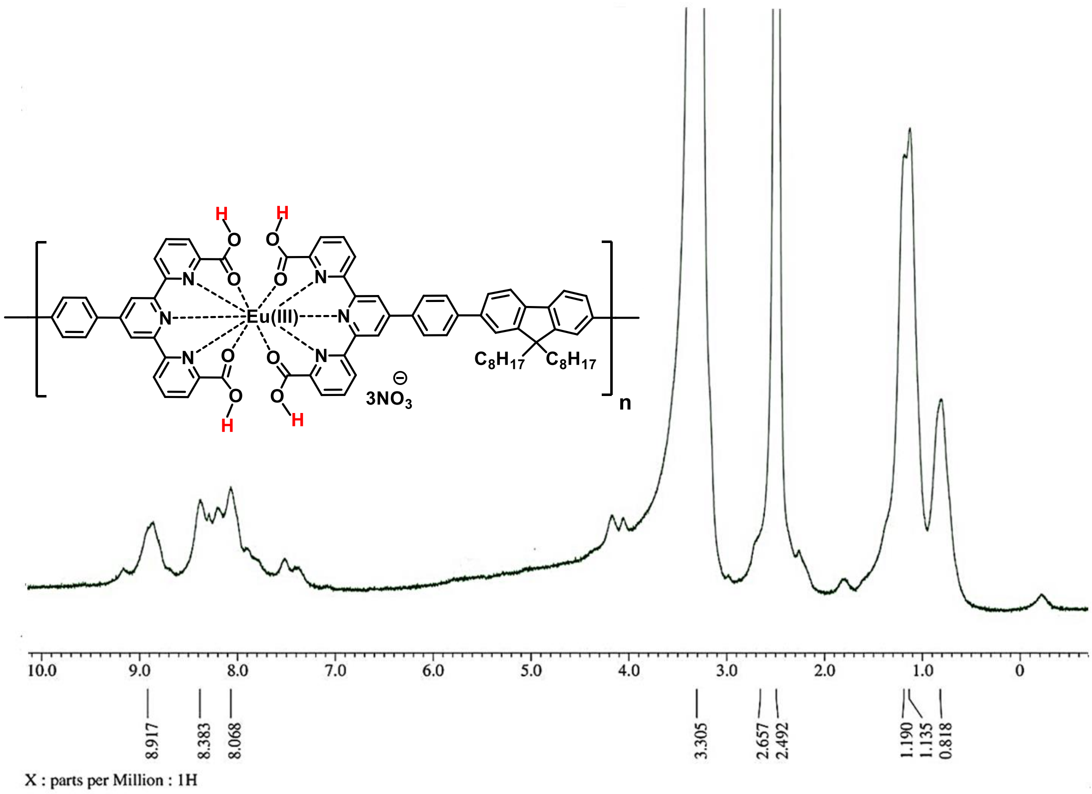

Fig. S11. ^{1}H NMR spectrum of **PolyEu-H**.

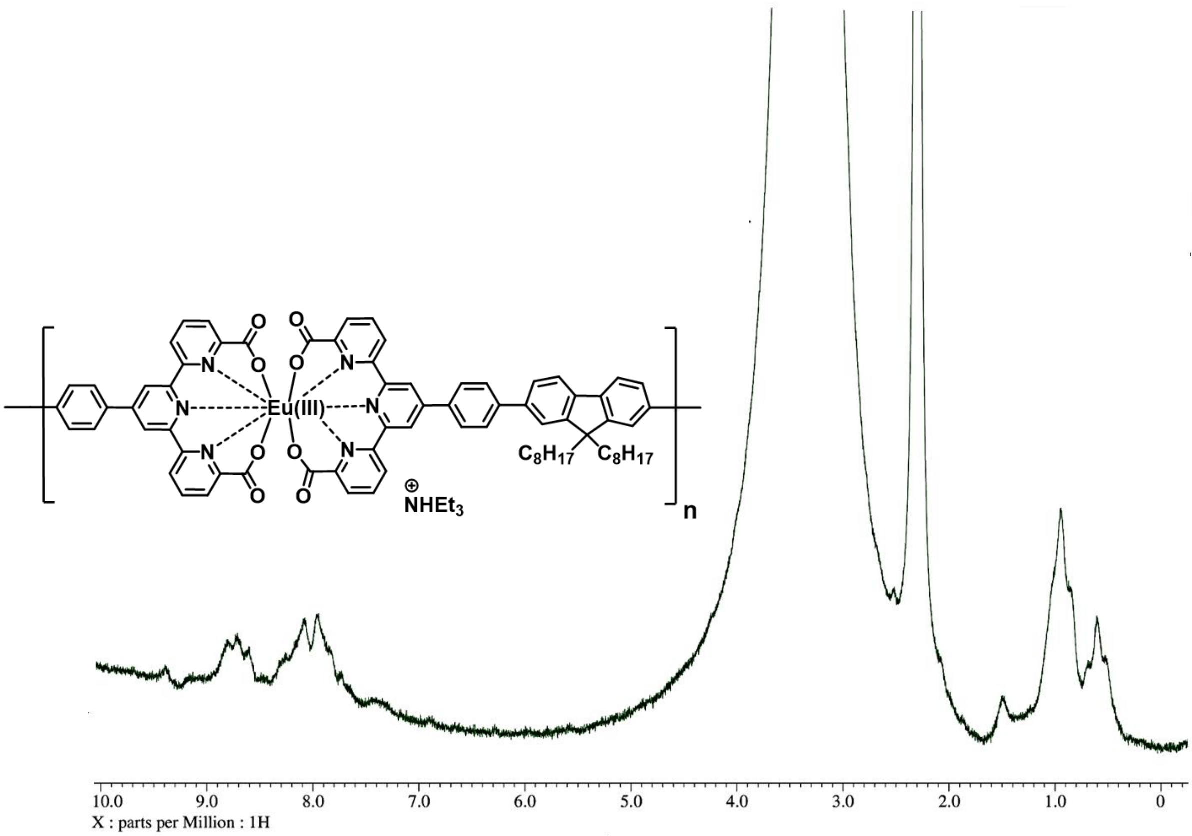

Fig. S12. ^{1}H NMR spectrum of **PolyEu**.

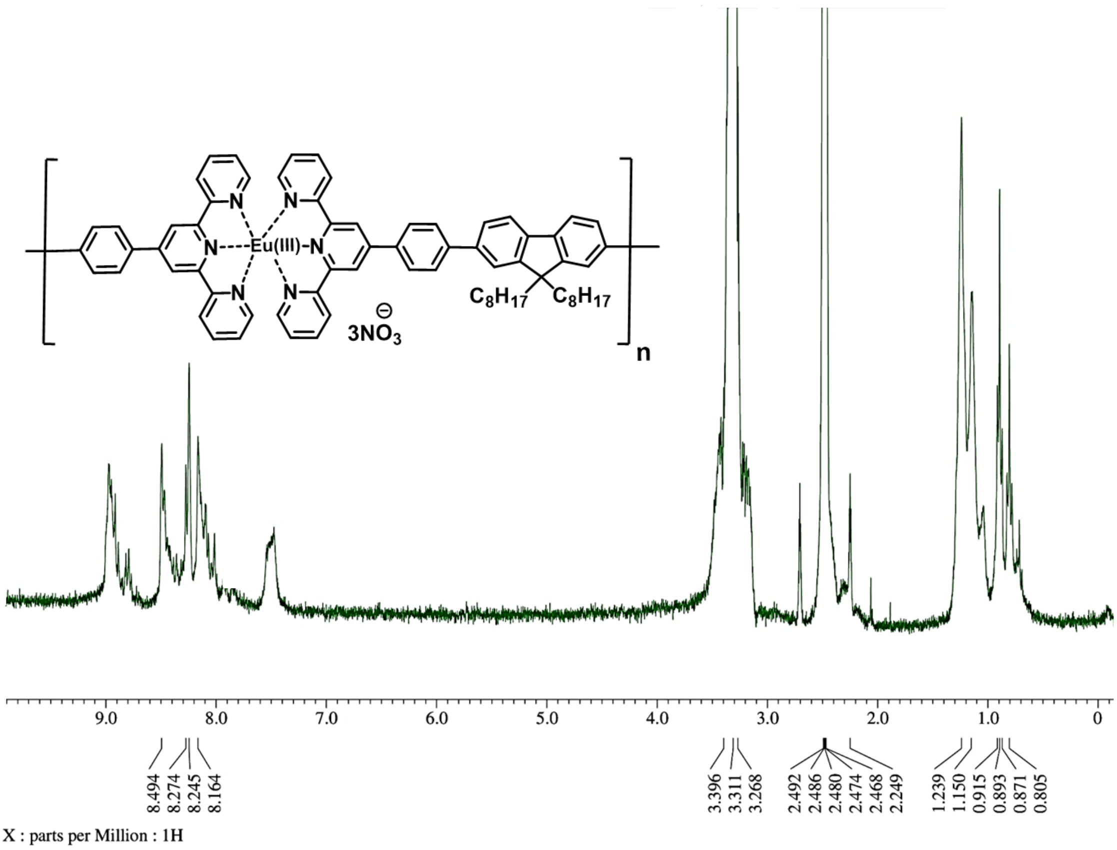

Fig. S13. ^{1}H NMR spectrum of **PolyEu-2**.

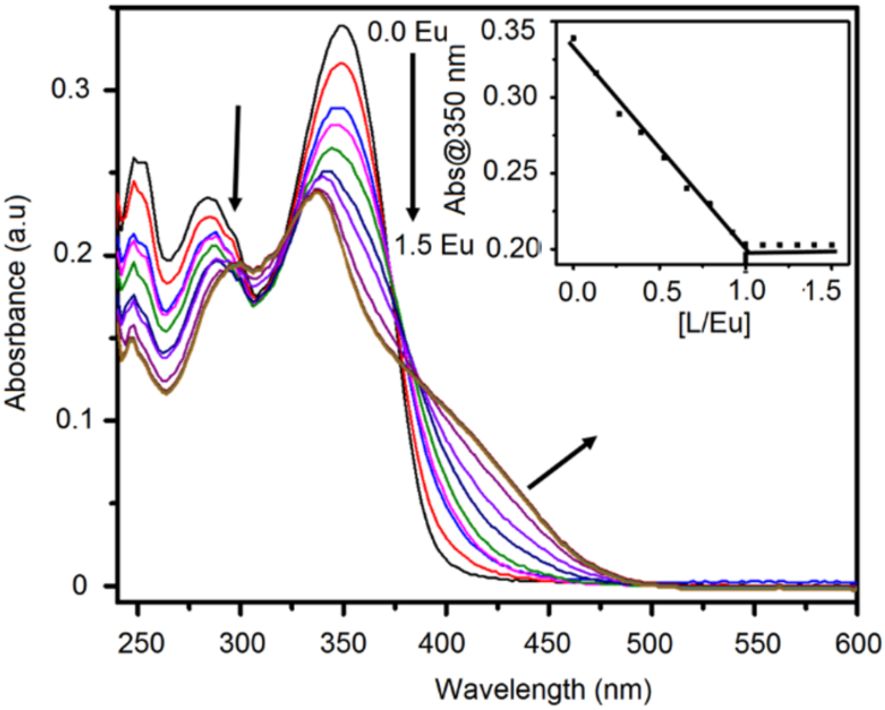

Fig. S14. a) The UV/Vis spectral change of L2 during the successive addition of $Eu(NO_3)_3.5H_2O$ (Inset: Absorption probed at 350 nm). (Solvent- $CHCl_3$/MeOH, Concertation-5µm)

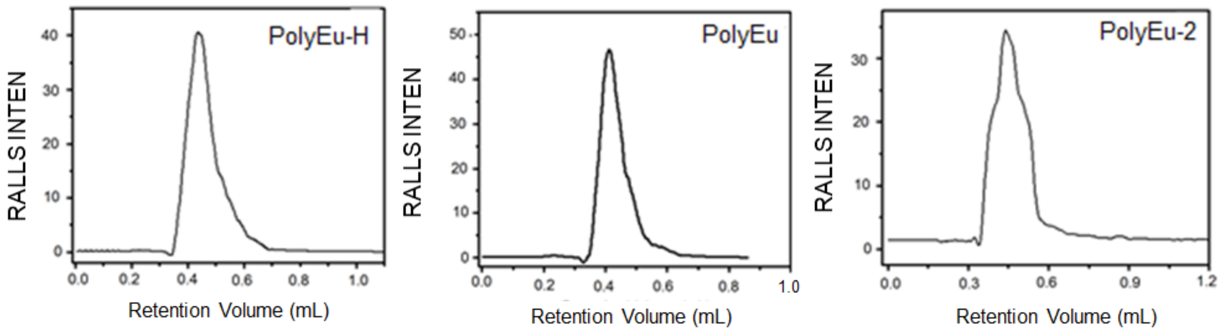

Fig. S15. The RALLS INTEN (INTEN = Intensity) change during the SEC-Viscometry-RALLS measurement of **PolyEu-H**, **PolyEu** and **PolyEu-2** in DMSO at room temperature.

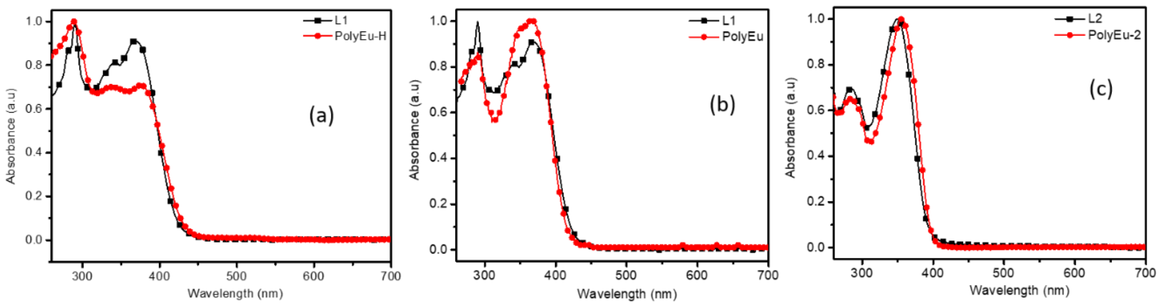

Fig. S16. a) The UV/Vis spectral change of ligands with their corresponding polymers in DMSO solvent (Normalized to 0-1). Concentration is ~ 1.25 mM

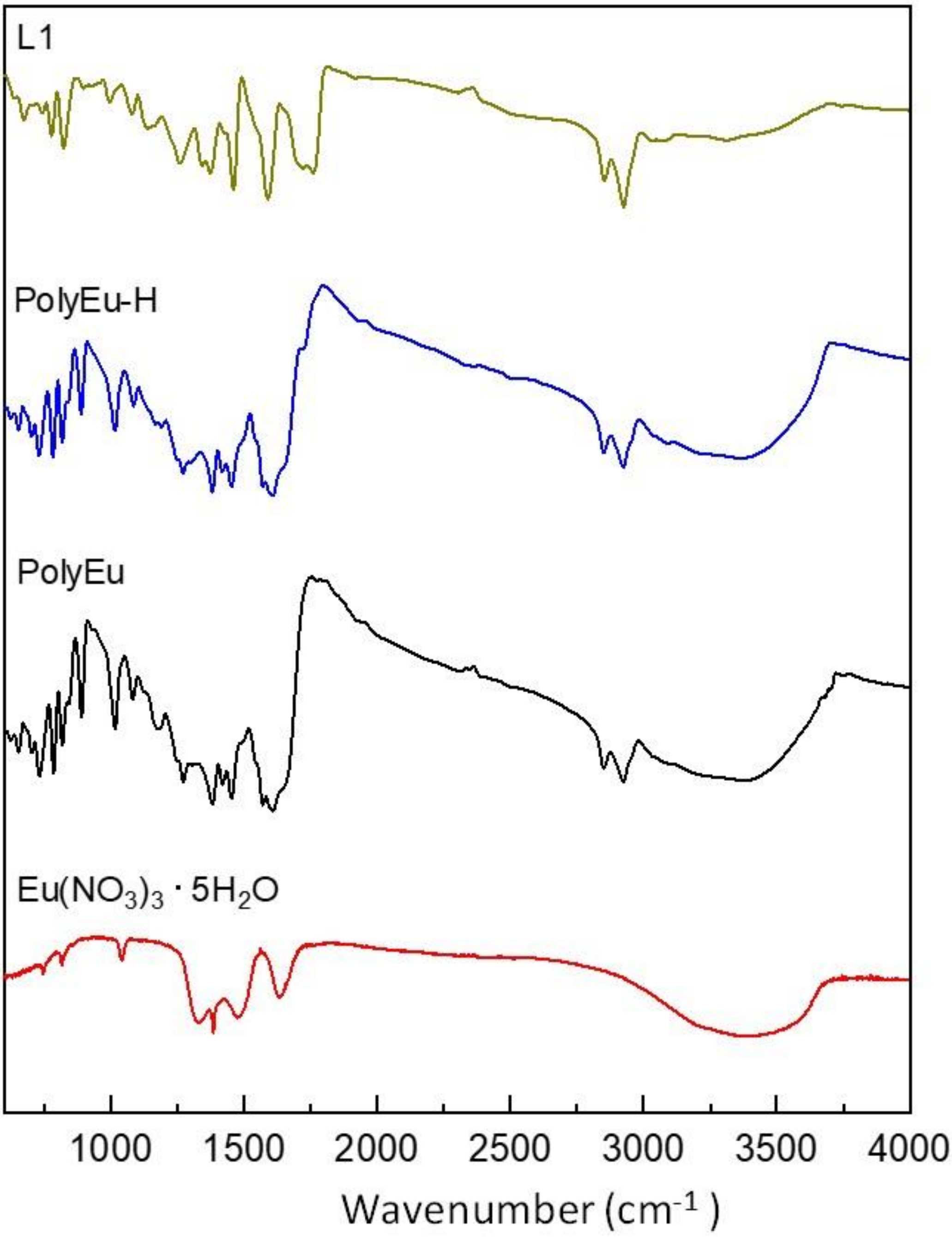

Fig. S17. FT-IR Spectra of L1, **PolyEu-H**, **PolyEu** and $Eu(NO_3)_3.5H_2O$

We showed FT-IR spectrum in the range of 600-2000 cm^{-1} in Fig. S17. We observe almost no difference in the fingerprint region of COOH (3700-2200).

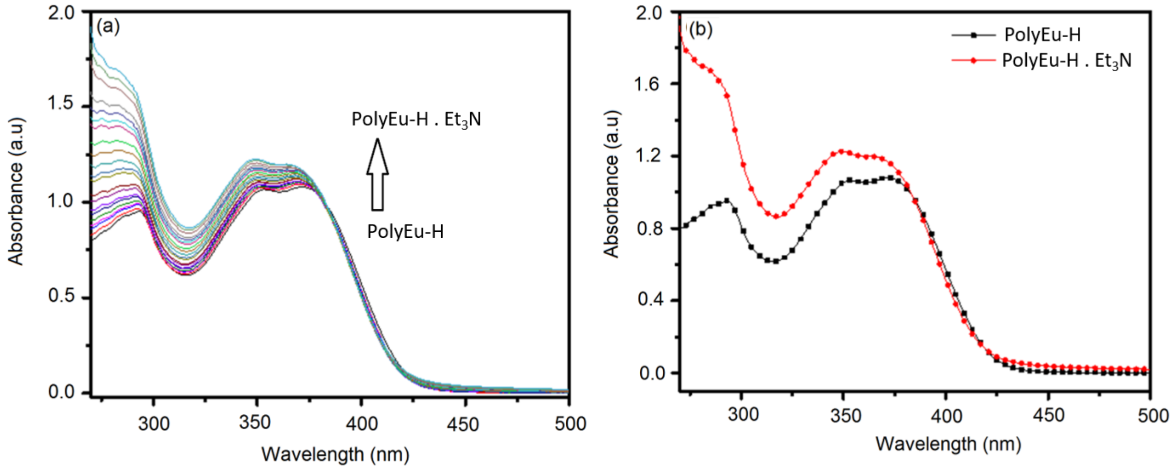

Fig. S18. Absorption changes of **PolyEu-H** on addition of triethylamine a) Absorption b) first and last specturum of (a).

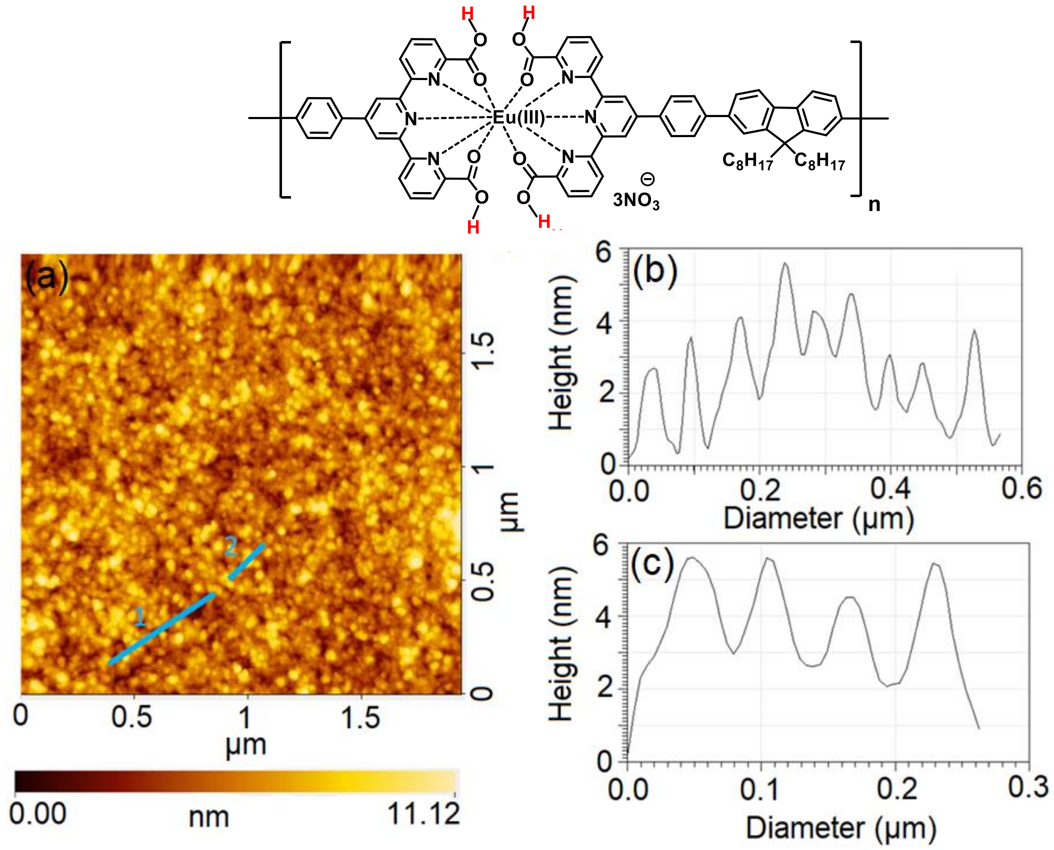

Fig. S19. a) AFM image of **PolyEu-H** b) and c) Diameter and height profile of line 1 and line 2 showed in fig a, respectively.

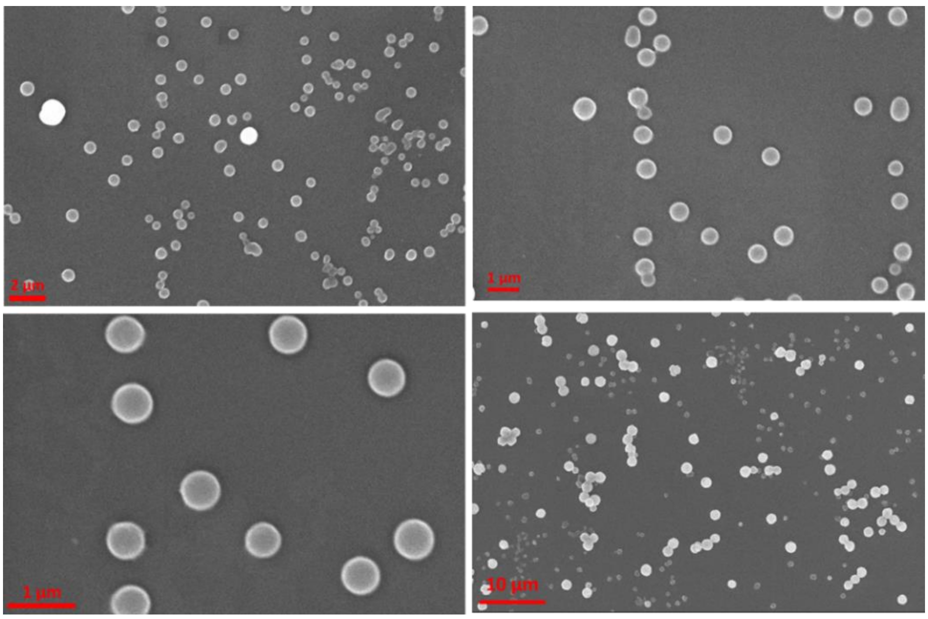

Fig. S20. a) Various magnified SEM images of **PolyEu-H**.

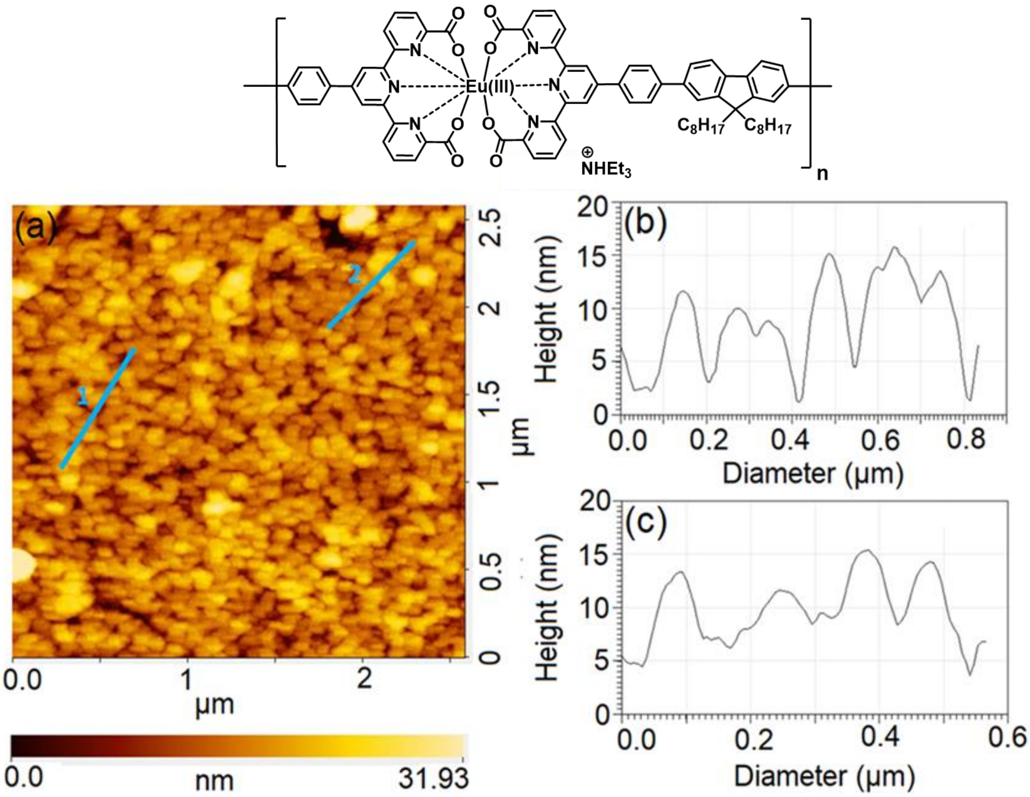

Fig. S21. a) AFM image of **PolyEu** b) and c) Diameter and height profile of line 1 and line 2 showed in fig a, respectively.

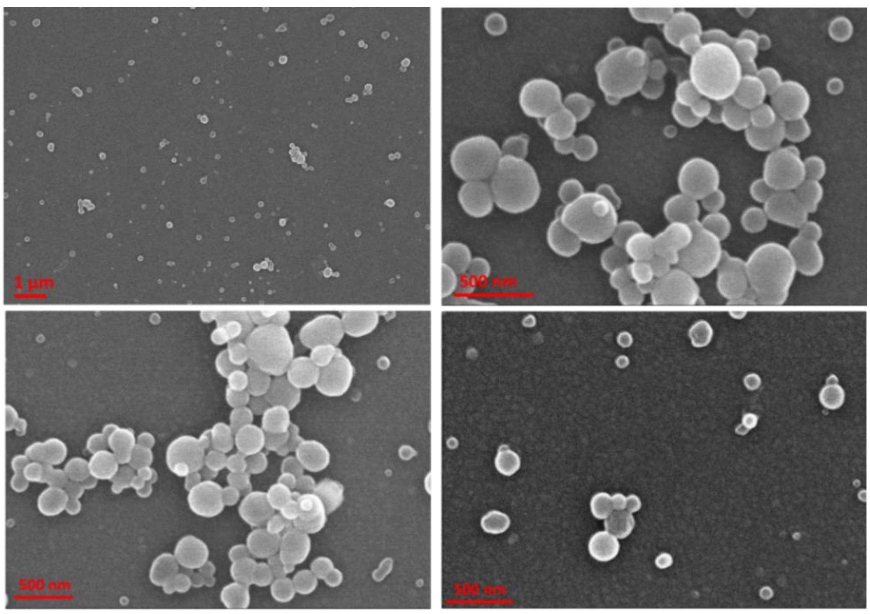

Fig. S22. a) Various magnified SEM images of **PolyEu**.

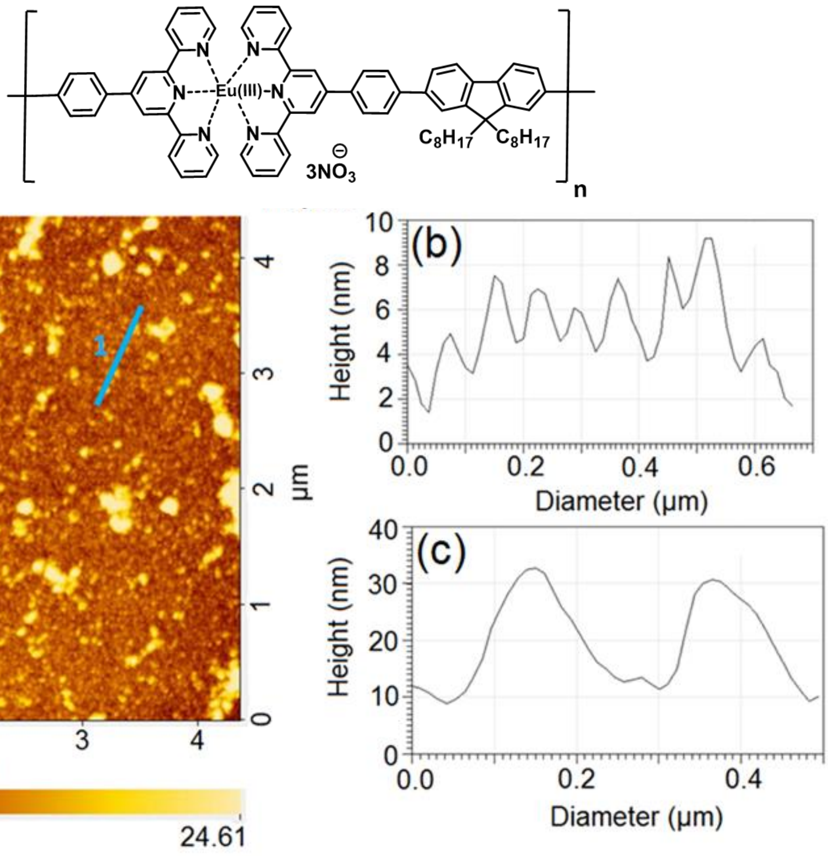

Fig. S23. a) AFM image of **PolyEu-2** b) and c) Diameter and height profile of line 1 and line 2 showed in fig a, respectively.

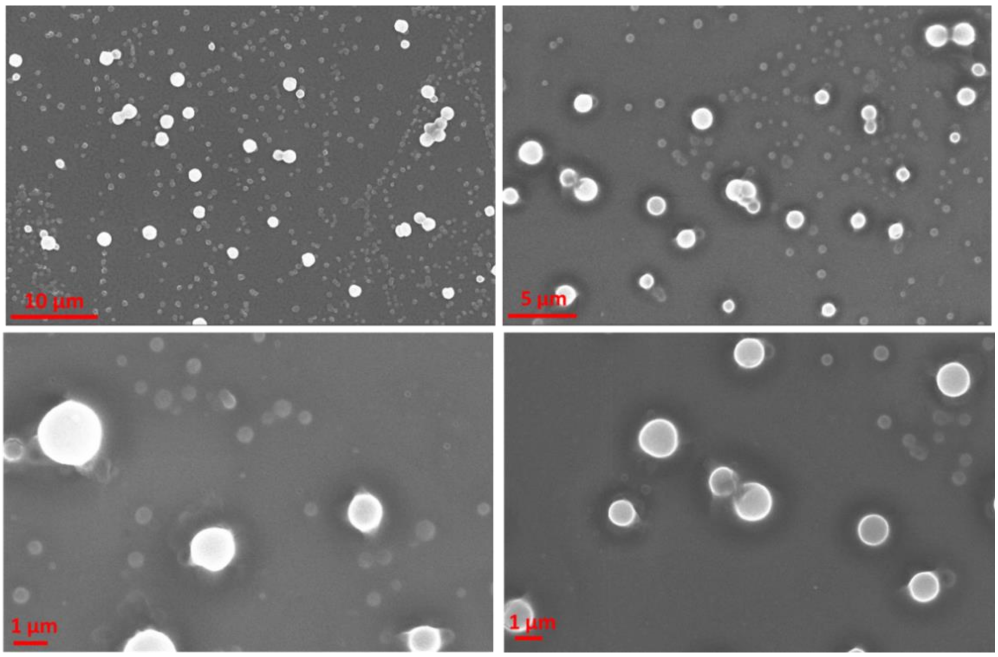

Fig. S24. Various magnified SEM images of **PolyEu-2**.

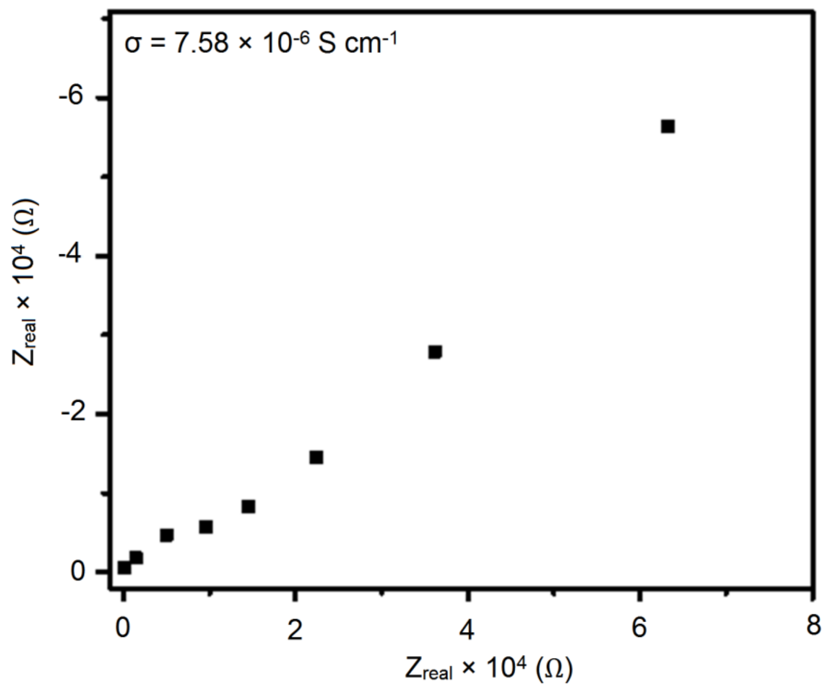

Fig. S25. The Nyquist plot for proton conductivity of **PolyEu** at 95% RH and 25 ^{o}C condition.

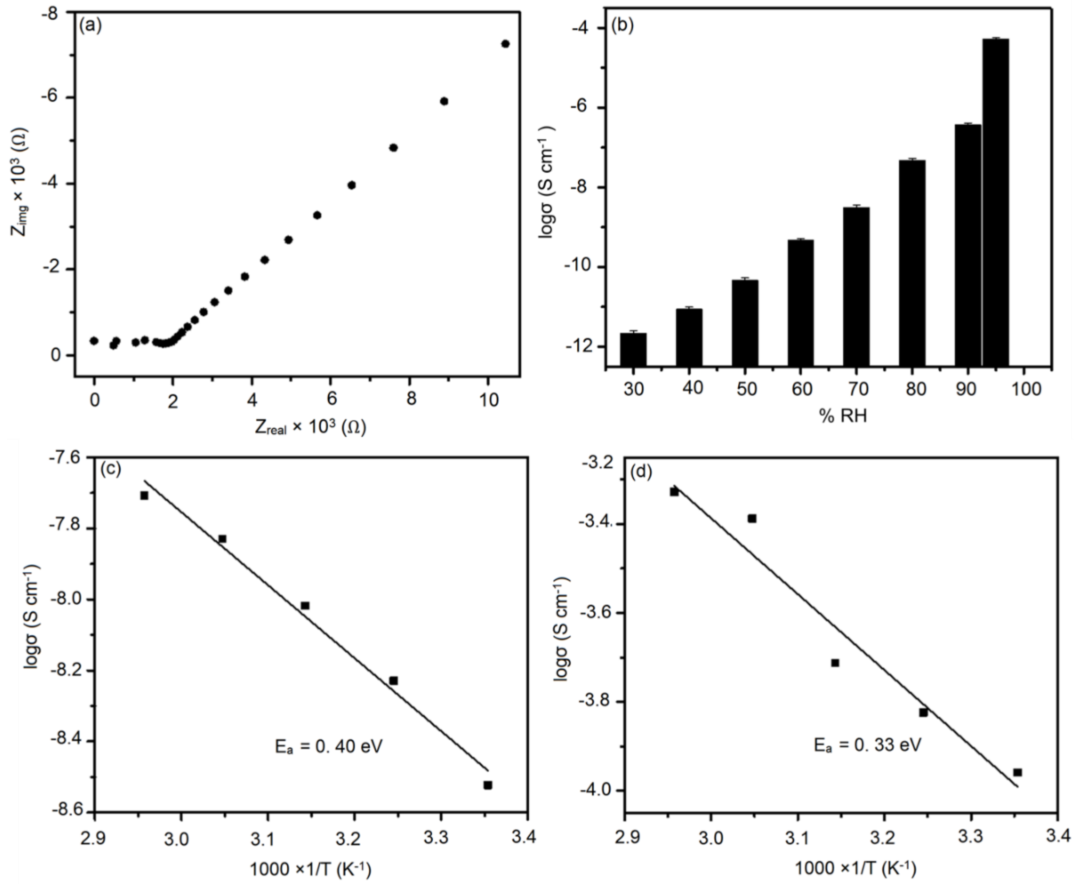

Fig. S26. a) The Nyquist plots for proton conductivity at 25 °C and 95% RH for **PolyEu-2** (frequency range: 1Hz to 30 MHz). b) Relation between the log (conductivity) and relative humidity of **PolyEu-2**. c) and d) Activation energy determination at 70% RH and 95% RH from Arrhenius plots for **PolyEu-2**.

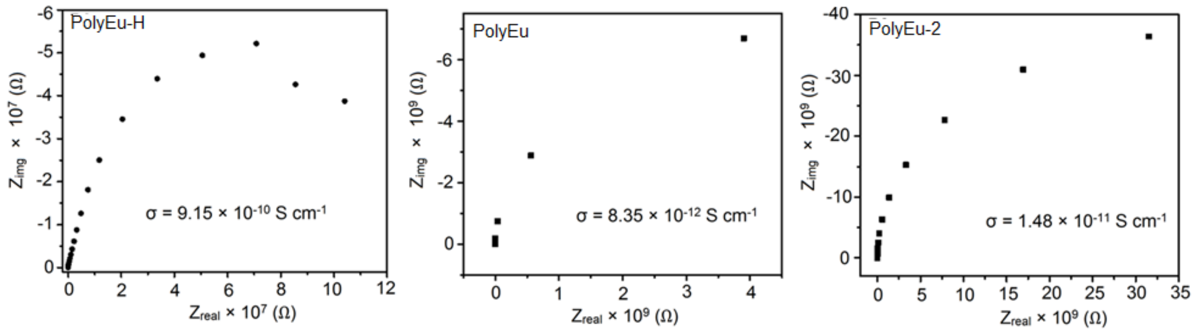

Fig. S27. The Nyquist plot for proton conductivity of (**polyEu-H**, **PolyEu**, and **PolyEu-2**) at 30% RH and 25 ^oC conditions.

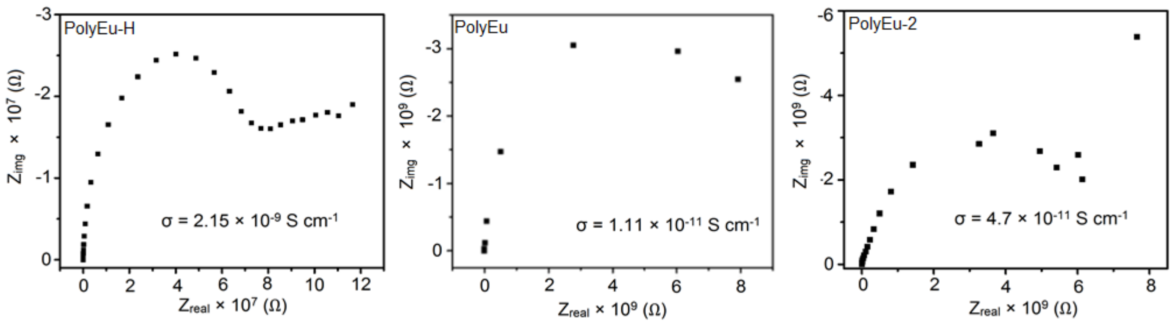

Fig. S28. The Nyquist plots for proton conductivity of (**polyEu-H**, **PolyEu**, and **PolyEu-2**) at 50% RH and 25 ^oC.

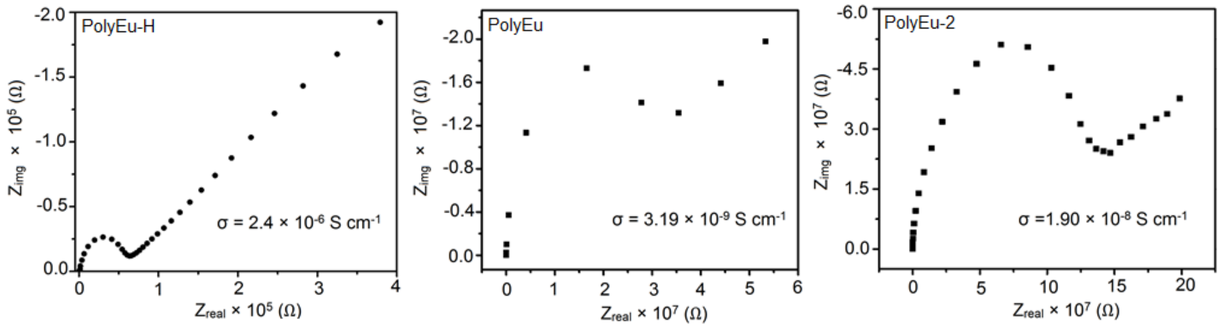

Fig. S29. The Nyquist plots for proton conductivity of (**polyEu-H, PolyEu and PolyEu-2**) at 70% RH and 25 ^{o}C.

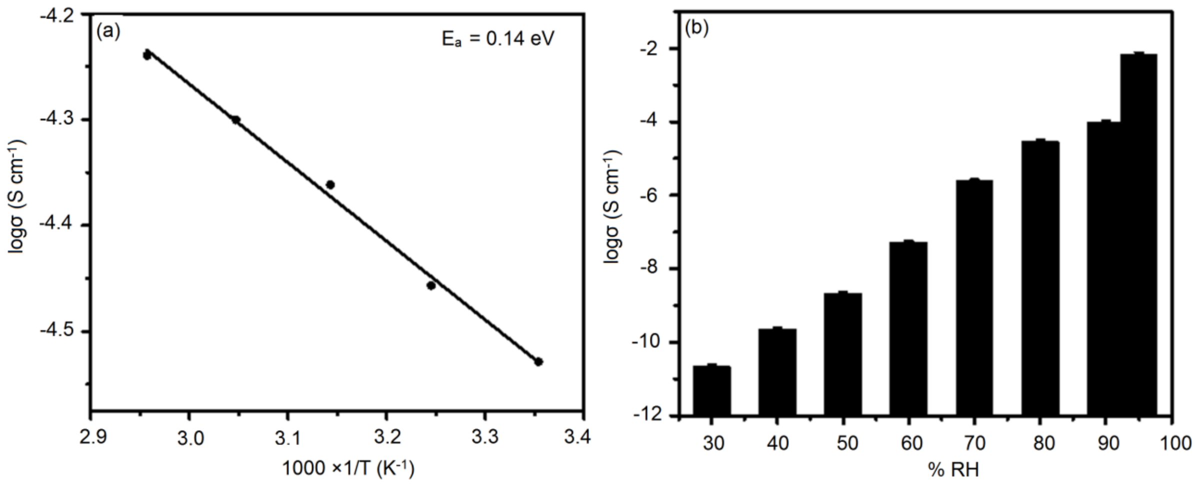

Fig. S30. a) Activation energy determination at 70% RH from Arrhenius plots for **PolyEu**. b) The relation between the log (conductivity) and relative humidity of **PolyEu**.

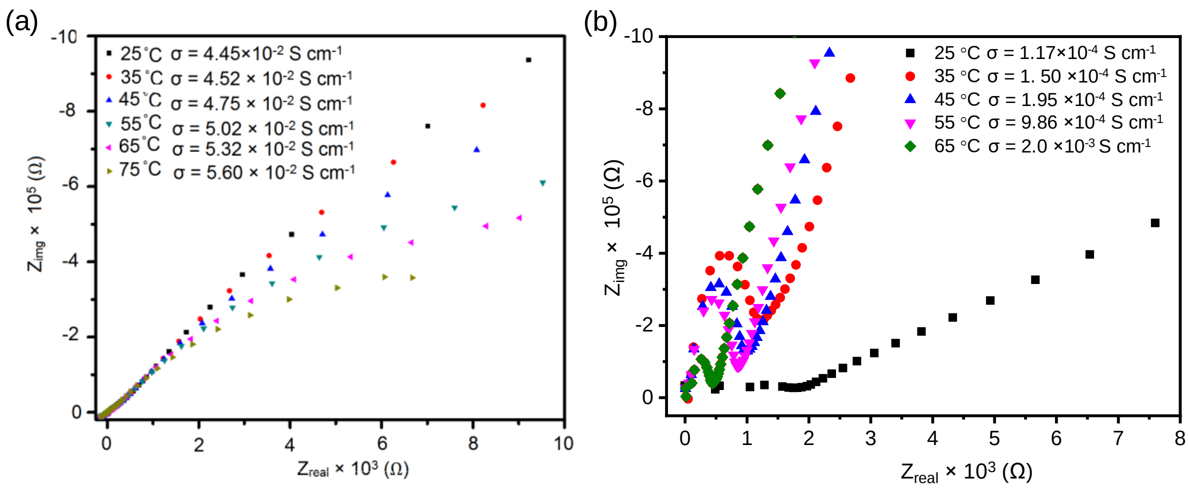

Fig. S31. The Nyquist plots for proton conductivity of **PolyEu-H** and **PolyEu-2** at 95% RH with different temperatures. a) **PolyEu-H** b) **PolyEu-2**.

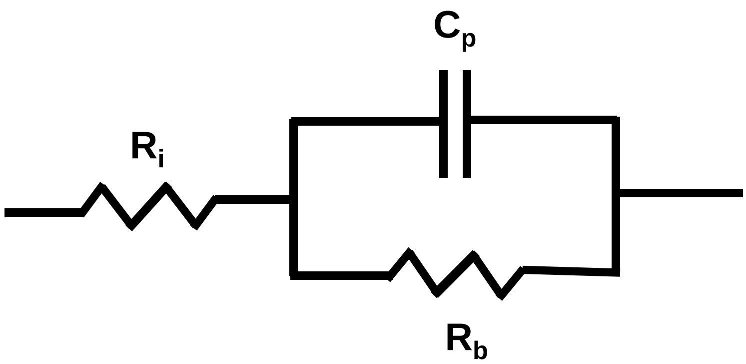

Fig. S32. Eqivalent circut used for fitting the impendance data from the Nquist plots

The Nyquist plot is not having semicircle, following equivalent circuit fitting is used to the impedance data (Fig. S32).

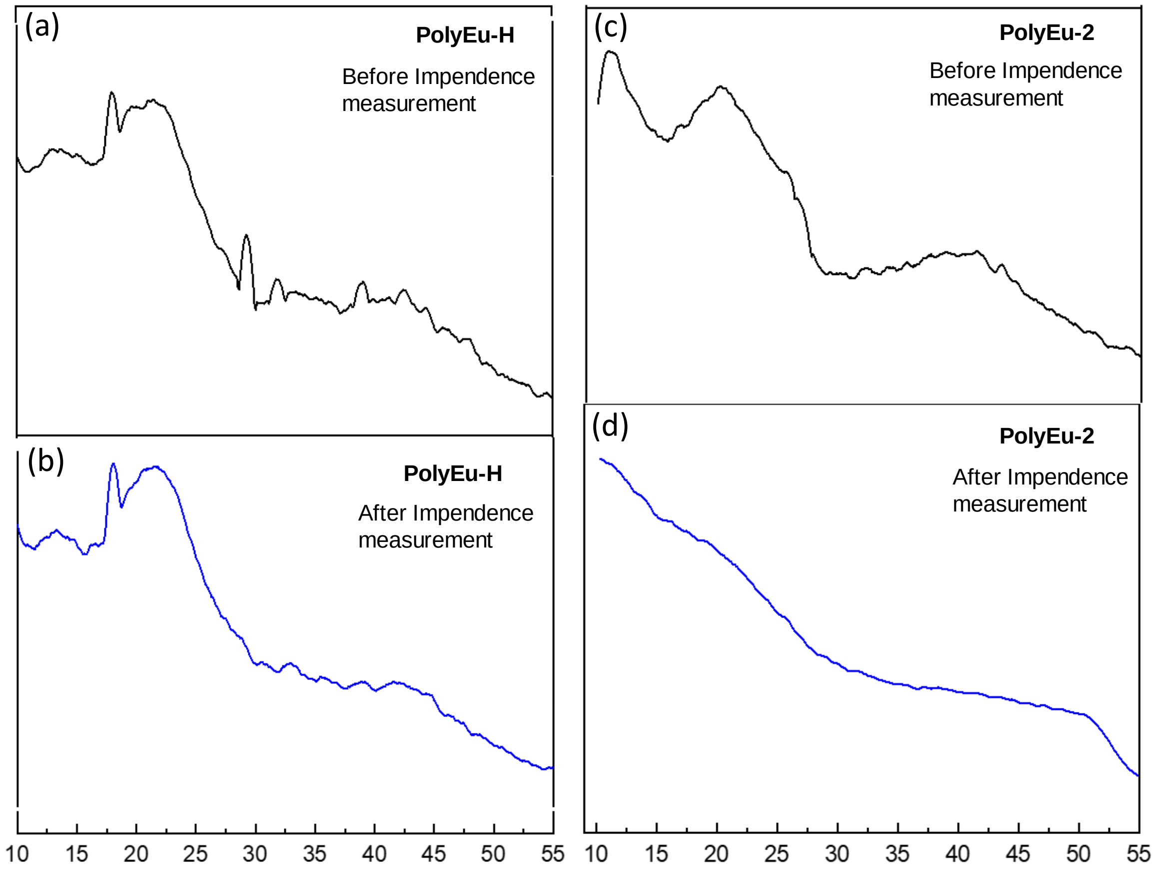

Fig. S33. The powder X-RD data of **PolyEu-H** and **PolyEu-2** before and after the impendance measurment a) **PolyEu-H** b) **PolyEu-2**

Fig.S33a showed the powder X-RD pattern of PolyEu-H before the impedance measurement.it is mostly like amorphous in nature. Fig. S33b showed X-RD pattern of PolyEu-H after the impedance measurement. There are no sharp peaks appeared. This result indicates crystallinity and decomposition of polymer not happened during the impedance measurement. Similarly, we also showed the powder X-RD pattern of polyEu-2 as a Fig. S33c (before the measurement) and d (after the measurement). We did not observe any kind of sharp peaks in Fig.33d. This clearly indicates polymer decomposition does not happened.

Table S1. Proton Conduction values of some reported porous crystalline Frameworks.

Compounds	**Conductivity (S cm^{-1})**	**Conditions**	**References**
HOF-GS-11	1.8×10^{-2}	25 ˚C, 95% RH	*Angew. Chem. Int. Ed.* **2016**, *55*, 10667–10671.
Fe-CAT-5	5.0×10^{-2}	25 ˚C, 98% RH	*J. Am. Chem. Soc.* **2015**, *137*, 15394–15397.
[(Me2NH2)3(SO4)]2[Zn2(ox)3]	4.2 x 10^{-2}	25 ˚C, 98% RH	*Angew. Chem. Int. Ed.* **2014**, *53*, 2638–2642.
(NH4)2(H2adp)[Zn2(ox)3]·3H2O	8.0 x 10^{-3}	25 ˚C, 98% RH	*J. Am. Chem. Soc.* **2009**, *131*, 9906-9907.
Ca-PiPhtA-NH3	6.6 x 10^{-3}	24 ˚C, 98% RH	*J. Am. Chem. Soc.* **2014**, *136*, 5731–5739.
Cu−TCPP nano-sheet	3.9 x 10^{-3}	25 ˚C, 98% RH	*J. Am. Chem. Soc.* **2013**, *135*, 7438-7441.
CB[6]·1.2H2SO4·6.4H2O (Organic based)	1.3 x 10^{-3}	25 ˚C, 98% RH	*Angew. Chem. Int. Ed.*, **2011**, *34*, 7870-7873.
CB[6]·1.1 HCl·11.3H2O (Organic based)	1.1 x 10^{-3}	25 ˚C, 98% RH	*Angew.Chem. Int. Ed.*, **2011**, *34*, 7870-7873.
PA@Tp-Azo (Organic based)	9.9×10^{-4}	25˚C, 98% RH	*J. Am. Chem. Soc.* **2014**, *136*, 6570-6573.
PolyEu-H	**4.4×10^{-2}**	**25˚C, 95% RH**	**This Work**

Table S2. Some known porous crystalline materials with very low activation energies.

Compounds	**E_a (eV)**	**References**
HOF-GS-11	0.13	*Angew. Chem. Int. Ed.* **2016**, *55*, 10667–10671
HPF2–100	0.10	*Adv. Mater. Interfaces* **2015**, *2*, 1500301
PA@Tp-Azo	0.11	*J. Am. Chem. Soc.* **2014**, *136*, 6570-6573.
H+@Ni2(dobdc)(H2O) 2 (pH = 1.8)	0.14	*Angew. Chem. Int. Ed.* **2014**, *53*, 8383–8387.
PCMOF-5	0.16	*J. Am. Chem. Soc.* **2013**, *135*, 1193-1196.
TfOH@MIL-101 0.18	0.18	*ACS Appl. Mater. Interfaces* **2014**, *6*, 5161-5167
[{(Zn0.25)8(O)}Zn6(L) 12(H2O)29 (DMF)69(NO3)2]n	0.22	*J. Am. Chem. Soc.* **2012**, *134*, 19432–19437.
PolyEu-H	**0.04**	**This Work**

Table S3. Proton Conduction and activation energies of some reported europium-based MOFs.

Compounds	**Conductivity ($S\ cm^{-1}$)**	**E_a (eV)**	**Conditions**	**References**
Eu-MOF	1.0×10^{-5}	0.91	25 ˚C, 97% RH	*Chem.Commun.* **2014**, *50*, 1912
Eu-MOF	1.1×10^{-3}	0.97	100 ˚C, 68% RH	*Chem.Commun.* **2014**, *50*, 9153
$Me_2NH_2][Eu(ox)_2(H_2O)]3H_2O$	2.73×10^{-3}	0.39	55 ˚C, 95% RH	*J. Mater. Chem. A*, **2016**, *4*, 16484
$(N_2H_5)[CeEu(C_2O_4)_4(N_2H_5)]\cdot 4H_2O$	3.42×10^{-3}	0.10	25 ˚C, 100% RH	*Adv. Mater.* **2017**, *29*, 1701804
$[Ln(H_4NMP)\text{-}(H_2O)_2]Cl\cdot 2H_2O$	2.0×10^{-3}	0.30	80 ˚C, 95% RH	*Inorg. Chem.* **2016**, *55*, 7414
PolyEu-H	**5.6×10^{-2}**	**0.04**	**75˚C, 95% RH**	**This Work**